2021 IEEE 4th International Conference on Automation, Electronics and Electrical Engineering (AUTEEE) | 978-1-6654-2839-2/21/$31.00 ©2021 IEEE | DOI: 10.1109/AUTEEE52864.2021.9668690

Error Compensation for Long Arm Manipulator Based on Deflection Modeling and Neural Network

Haoying Li
College of Control Science and Technology, Zhejiang University
Huzhou Research Institute of Zhejiang University
Hangzhou, China
lhy18735@163.com

Chenhao Fang
College of Control Science and Technology, Zhejiang University
Hangzhou, China
fang_chenhao@foxmail.com

Jinze Shi
College of Mechanical Engineering, Zhejiang University
Hangzhou, China
3180104797@zju.edu.cn

Baocheng Zeng
College of Control Science and Technology, Zhejiang University
Hangzhou, China
3180102361@zju.edu.cn

Chunlin Zhou*
College of Control Science and Technology, Zhejiang University,
Huzhou Research Institute of Zhejiang University
Hangzhou, China
c_zhou@zju.edu.cn

***Abstract*—Long arm manipulators are designed to work in special conditions including aviation, engineering, and other scenarios that require a large span operation. However, since the long arm will cause a large flexible error, the manipulators maintain large terminal absolute error and difficulty in control. In addition, testing in a real machine is time and economic consuming, and obtaining enough data is untoward. Under such conditions, this paper proposes an error compensation method for a long arm manipulator combining deflection error modeling and neural network, using a specially designed long arm manipulator. By using this method, better results are achieved than traditional error modeling alone since non-traceable errors are also compensated for. The result is also better than neural network compensation alone since in the case of less training data preferable results can still be achieved.**

Keywords—manipulator, deflection, neural network, absolute error compensation

I. INTRODUCTION

Many working scenarios require the special configuration of the manipulator with the long arm. Such applications include aviation fields such as Canadarm [1], American Space Arm [2], construction machinery such as Rock Drilling Machine [3]. The long arm manipulator has a large working space, but the control is more difficult, with larger errors of absolute end positioning, because long arm manipulators have a heavy load, large span, and joint redundancy, leading to rigid-flexible coupling and significant deflection deformation.

The traditional manipulator error compensation scheme is DH calibration, which can compensate for errors caused by manufacturing and assembly. Some methods to improve the accuracy and speed of DH calibration are also raised. Newman [4] used the laser tracker to correct structural parameters. Nicolas [5] used a camera and fixed error compensation plate on the 6-axis parallel machine. While the accuracy of normal manipulators can meet the requirement after DH calibration, it is not enough for long arm manipulators.

In allusion to the low accuracy of long arm manipulators caused by large flexibility errors, many researchers proposed solutions. Some researchers estimate and model the deflection error. Khalil et al. [6] used a special Newton-Euler recursive algorithm to obtain the flexible transfer matrix. Huang Kaifeng et al. [7] took the deformation of the drilling arm as a virtual joint. Wang et al. [8] used the dual quaternion method to model the inverse solution. The theoretical derivation is interpretable, but the calculation is complex and factor-deficient. Jie et al. [9] obtained the flexibility error based on machine vision and laser ranging. Benallegue et al. [10] used an inertial measurement unit to measure the influence of gravity and inertia on the joints. The measured errors accord with the real but need the support of the precise equipment. Another kind of method is to use a neural network to predict the error. Tan et al. [11] proposed the pseudo target point method based on BP neural network. Wang et al. [12] used BP neural network optimized based on a genetic algorithm to finish compensation. The neural network can compensate for the untraceable error, but it is difficult to collect a large amount of data in real working conditions, and insufficient data sets will lead to inaccurate compensation.

To solve the problems mentioned above, this paper proposes an end error compensation scheme based on deflection error modeling and neural network predicting error, which under the circumstances of the fewer amount of data in the neural network can still get good compensation results. The remainder of this article is organized as follows: Section II introduces the overview of the compensation method first. Then the establishment of deflection error model and compensation based on backpropagation neural network optimized by sparrow search algorithm is introduced in detail. Section III presents the experiment of the method. Section IV summarizes the paper.

II. ERROR COMPENSATION

A. Overview of Error Compensation Method

Due to the high cost of the real manipulator test in engineering application scenarios, the long arm manipulator is primarily established in this paper to simulate the large deflection manipulator in real working conditions.

Authorized licensed use limited to: Zhejiang University. Downloaded on April 27,2022 at 09:15:53 UTC from IEEE Xplore. Restrictions apply.

The study uses an improved DH modeling method (MDH) [13] to build the kinetic model. In the establishment of an inverse kinematics solver, considering the special configuration of the manipulator, the study adopts a numerical solution scheme. The Newton-Raphson iterative method is used in this study, which has the advantage of the simple program and fast convergence.

For any large deflection manipulator, the implementation process of this method is as follows. Firstly, the system will check whether the manipulator is a new operation object. If it is a new manipulator, the DH parameter table should be constructed according to its structure. Based on the establishment of the manipulator model, the next step is preprocessing. The pretreatment includes two parts. Firstly, DH calibration is conducted to reduce the variation of kinematic parameters and joint zero deviation due to the inaccuracy of parts manufacturing and assembly. Then, neural network training is performed containing data collection and network training. After the pre-processing, further error compensation can be carried out.

The further compensation in the study contains mainly two parts. Firstly, the deflection deformation caused by the connecting rod's weight is modeled, and then the forward and inverse kinematics solver is modified with the large deflection error factor added. The detailed correction process will be described specifically later.

After the deflection error is considered by the solver, the residual error is estimated by the neural network. In this study, a sparrow search-optimized Back-Propagation neural network (SSA-BP) is adopted to predict the position error of the manipulator end. For the target points input by users, the ideal joint angles are firstly obtained by using the inverse kinematics with deflection error factors, and then the ideal joint angles are input into the neural network trained in advance to obtain the estimated error of end positioning. The sum of the target point value and the predicted error is considered to be the new target point, and the inverse kinematics solver is input for the second time to get the executed angle, which is used to control the motor.

Through this process, A universal end-position error compensation scheme for long arm manipulator is proposed. Errors caused by large deflection can be solved on the one hand, and errors that are difficult to trace can be remedied on the other hand.

B. Deflection Error Model

Since the deflection error caused by gravity is the main error source of the long-arm manipulator, the error caused by large deflection should be compensated first. In this paper, the solver is directly transformed with the deflection factor added.

The transmission relation of deflection error between adjacent links is established. The relation between the actual transformation matrix and the ideal transformation matrix is shown in Equation (1).

$$ {}^{i-1}_{i}T' = {}^{i-1}_{i}T + dT_i \tag{1}$$

where ${}^{i-1}_{i}T'$ is the actual transformation matrix between coordinate systems; ${}^{i-1}_{i}T$ is the ideal transformation matrix between coordinate systems; $\mathrm{d}T_i$ is the error between the real and ideal transformation coordinate systems, which can be obtained by differential approximation in Equation (2).

$$ \mathrm{d}T_i = {}^{i-1}_{i}T \cdot \Delta_i \tag{2}$$

where Δ_i is the position error matrix of the adjacent link coordinate system, which is shown in Equation (3).

$$ \Delta_i = \begin{bmatrix} 0 & -\delta_{iz} & \delta_{iy} & d_{ix} \\ \delta_{iz} & 0 & -\delta_{ix} & d_{iy} \\ -\delta_{iy} & \delta_{ix} & 0 & d_{iz} \\ 0 & 0 & 0 & 0 \end{bmatrix} \tag{3}$$

where $[\delta_{ix} \quad \delta_{iy} \quad \delta_{iz}]$ and $[d_{ix} \quad d_{iy} \quad d_{iz}]$ represent the attitude error and position error of the coordinate system Σ_i relative to Σ_{i-1}. The deflection error modeling is realized by deducing the pose error matrix of adjacent links under the deflection effect.

The flexible deformation of connecting rod can be simplified to a cantilever beam model. And the terminal coordinate system of the connecting rod before and after deformation is shown in Fig. 1.

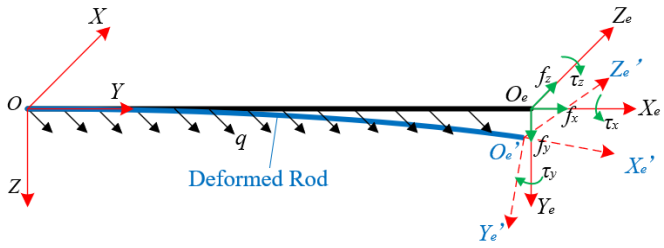

Fig. 1. Diagram of end coordinate system before and after deformation

Each link is exerted by three kinds of effect, including a uniformly distributed dead weight, the terminal force exerted by the gravity of subsequent links, and the terminal torque caused by the gravity of subsequent links. According to the reference [14], through force analysis, the differential motion vector of the deformed connecting rod end coordinate system can be deduced, and then the value of $[\delta_{ix} \quad \delta_{iy} \quad \delta_{iz}]$ and $[d_{ix} \quad d_{iy} \quad d_{iz}]$ can be attained.

Next, the errors caused by the deflection at the end of the manipulator are derived. The standard form of the terminal pose formula is shown in (5).

$$ T_i = {}^{i-1}_{i}T\,{}^{i}_{i+1}T \cdots {}^{n}_{n+1}T = \begin{bmatrix} \boldsymbol{n_i} & \boldsymbol{o_i} & \boldsymbol{a_i} & \boldsymbol{p_i} \\ 0 & 0 & 0 & 1 \end{bmatrix} \tag{4}$$

Accordingly, the terminal differential motion of the connecting rod caused by the flexible deformation is shown as Equation (5).

$$ \mathrm{D} = \begin{bmatrix} d_x \\ d_y \\ d_z \\ \delta_x \\ \delta_y \\ \delta_z \end{bmatrix} = \sum_{i=1}^{n+1} \begin{bmatrix} (\boldsymbol{n_{i+1}})^T & (\boldsymbol{p_{i+1}} \times \boldsymbol{n_{i+1}})^T \\ (\boldsymbol{o_{i+1}})^T & (\boldsymbol{p_{i+1}} \times \boldsymbol{o_{i+1}})^T \\ (\boldsymbol{a_{i+1}})^T & (\boldsymbol{p_{i+1}} \times \boldsymbol{a_{i+1}})^T \\ \boldsymbol{0_{1\times3}} & (\boldsymbol{n_{i+1}})^T \\ \boldsymbol{0_{1\times3}} & (\boldsymbol{o_{i+1}})^T \\ \boldsymbol{0_{1\times3}} & (\boldsymbol{a_{i+1}})^T \end{bmatrix} \begin{bmatrix} d_{ix} \\ d_{iy} \\ d_{iz} \\ \delta_{ix} \\ \delta_{iy} \\ \delta_{iz} \end{bmatrix} \tag{5}$$

According to the above formula, the relationship between input joint angles and corresponding terminal prediction errors can be obtained. And the calculation of deflection error can be added to the solution of forward and inverse kinematics.

Authorized licensed use limited to: Zhejiang University. Downloaded on April 27,2022 at 09:15:53 UTC from IEEE Xplore. Restrictions apply.

C. Error Compensation Based on Back Propagation Neural Network Optimized by Sparrow Search Algorithm

Sparrow search algorithm (SSA) [15] [16] is a new intelligent optimization algorithm invented in 2020, which has high performance in different search Spaces and can explore potential global optimal regions.

SSA is a swarm optimization algorithm inspired by sparrow foraging and anti-predation behavior. During the foraging process, the sparrow population is divided into two parts, explorers and followers, which are responsible for providing the foraging direction of the population and following and obtaining food respectively.

In the SSA, the discoverers with better values have priority to obtain food in the search process. During each iteration, the location of the discoverer is updated as below:

$$X_{i,j}^{t+1} = \begin{cases} X_{i,j}^{t} \cdot exp\left(\frac{-i}{\alpha \cdot iter_{max}}\right) & if\ R_2 < ST \\ X_{i,j}^{t} + Q \cdot L & if\ R_2 \geq ST \end{cases} \quad (6)$$

where t indicates the current iteration, d shows the dimension of variables and $j = 1, 2, \ldots, d$. $X_{i,j}^{t}$ represents the value of the jth dimension of the ith sparrow at iteration t. $iter_{max}$ is a constant with the largest number of iterations. $\alpha \in (0, 1]$ is a random number. R_2 ($R_2 \in [0, 1]$) and ST ($ST \in [0.5, 1.0]$) represent the alarm value and the safety threshold respectively. Q is a random number that obeys normal distribution. L shows a matrix of $1 \times d$ for which each element inside is 1. Some followers will always observe the discoverer during the foraging process. The updated description of the followers' location is as follows:

$$X_{i,j}^{t+1} = \begin{cases} Q \cdot exp\left(\frac{X_{worst}^{t} - X_{i,j}^{t}}{\alpha \cdot iter_{max}}\right) & if > n/2 \\ X_{i,j}^{t+1} + \left|X_{i,j}^{t} - X_{p}^{t+1}\right| \cdot A^{+} \cdot L & otherwise \end{cases} \quad (7)$$

where X_p is the optimal position currently occupied by the discoverer, and X_{worst} is the current global worst position. A denotes a matrix where each element is randomly assigned a value of 1 or -1, and $A^{+} = \boldsymbol{A^{T}(AA^{T})^{-1}}$.

The location update of the vigilantes is described as follows:

$$X_{i,j}^{t} = \begin{cases} X_{i,j}^{t} + K \cdot exp\left(\frac{|X_{worst}^{t} - X_{i,j}^{t}|}{(f_i - f_w) + \varepsilon}\right) & if f_i = f_g \\ X_{best}^{t} + \beta \cdot \left|X_{i,j}^{t} - X_{best}^{t}\right| & if\ f_i > f_g \end{cases} \quad (8)$$

where X_{best} is the current global optimal position. As the step control parameter, β is a random number that obeys a normal distribution with mean 0 and variance 1. $K(K \in [-1,1])$ is a random number, and f_i is the fitness value of the current sparrow. f_g and f_w are the current global best and worst fitness values. ε is a constant to avoid 0 in the denominator.

BP network contains an input layer, an output layer, and some hidden layers. The update of its weights and bias is the most crucial step in its whole learning process. The SSA has the advantage of avoiding the optimum local problem. Therefore, it is used to optimize the BP.

The SSA is used to optimize the BP for getting the optimal weights and bias. The initialization of parameters in SSA includes the number of sparrow populations, the proportion of discoverers, the warning value, the maximum number of iterations. After the initialization of the input layer, the hidden layer and the output layer, the SSA is then used to search for optimal weights and bias. The fitness function of the SSA can be set as the neural network's error function according to the error in the optimization process.

The optimization process can be further explained as follows. Firstly, calculate the sparrow's fitness value, and determine its extreme value and the global optimal extreme value. Secondly, use Equation (6)(7)(8) to update the sparrow's position, and obtain the updated value of the sparrow's fitness. Thirdly, repeatedly update the sparrow's individual extreme and global extreme value according to the new fitness values. Fourthly, return to step two if the expected condition is not met. Finally, the SSA is finished when the error reaches the desired value, or the iteration number reaches the set maximum number. At this time, the weights and biases of the BP are set according to the obtained optimal results.

In this study, the scheme of changing the input target point by neural network mainly refers to the references [11] [12]. The command joint angle was taken as input during the training set collection, and the difference between the real position obtained by the binocular camera and the ideal position obtained by forward kinematics correction was taken as output.

The network was pre-trained and saved. When the user gives the target position, the angle is obtained by solving the improved inverse kinematics first. Then the angle will be input in the pre-trained network to get the corresponding predicted error. Then add the user target point and the predicted error to get the new target position. This modified target position is solved by improved inverse kinematics again, finally, the obtained angle will be input to the steering gear.

III. EXPERIMENT

A. Establishment of Long-arm Manipulator Model

Due to the high cost of real engineering machinery experiments, we designed a simplified manipulator with large deflection for researchers to carry out experiments, and the model has universality.

The parameters of the manipulator in the experiment are geometrically quantified by the real rock drilling machine, which is shown in Fig. 2.

The abstract model of the long arm manipulator is shown in Fig. 3. The manipulator module consists of five rotating joints and two prismatic joints. The last joint can be pre-specified as an appropriate degree of freedom for needle-like forward excavation according to the actual machine. To conform to the real situation and facilitate future engineering applications, the last fixed value of the joint was tested. However, by changing the DH parameters, this scheme can be easily extended to any large deflection manipulator.

Authorized licensed use limited to: Zhejiang University. Downloaded on April 27,2022 at 09:15:53 UTC from IEEE Xplore. Restrictions apply.

Fig. 2. Rock Drilling Machine

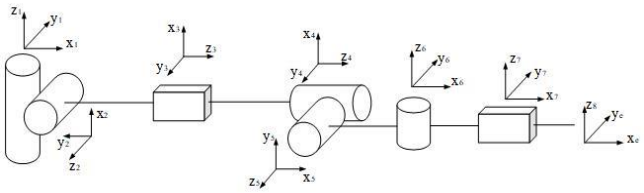

Fig. 3. Abstract Model of the Manipulator

The study uses 3D printing to obtain the mechanical arm, and its simulation picture and real mechanical arm are respectively shown in Fig. 4.

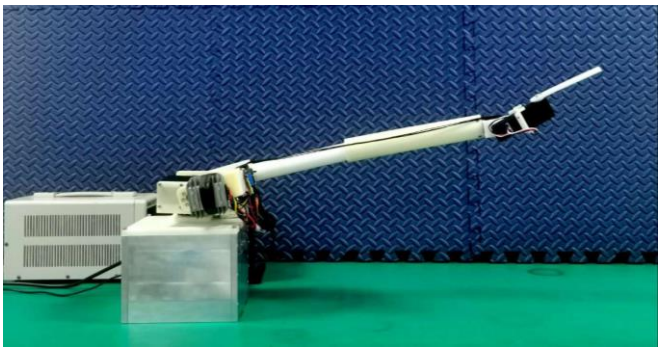

Fig. 4. Manipulator for Experiment

B. The Source of Data

SSA-BP compensates networks require pre-training. The training set was collected into 5 groups. The detailed data set process is as follows. 3 values of 5 rotation joints in each group were combined, and the values are chosen to accomplish the maximum variation value of angle which within the range that the binocular camera could read. Prismatic joints include joint 3 and joint 7. Five evenly distributed combinations from the shortest to the longest were selected. The training set is illustrated in Fig. 5.

The specific values are as follows: the angles of joint 1 include -15°, 0°, 15°; the angles of joint 2 include 0°, 15°, 30°; the angles of joint 4 include 0°, 30°, 60°; the angles of joint 5 include -45°, -25°, 0°; the angles of joint 6 include -30°, 0°, 30°; the combination of length of prismatic joint 3 and prismatic joint 7 include 0 mm and 0 mm, 0 mm and 63 mm, 60 mm and 10 mm, 53 mm and 63 mm, 104 mm and 18 mm, 105 mm and 63 mm.

During the error compensation test, 40 target points were randomly generated for testing. All control groups used the same test points to avoid other factors.

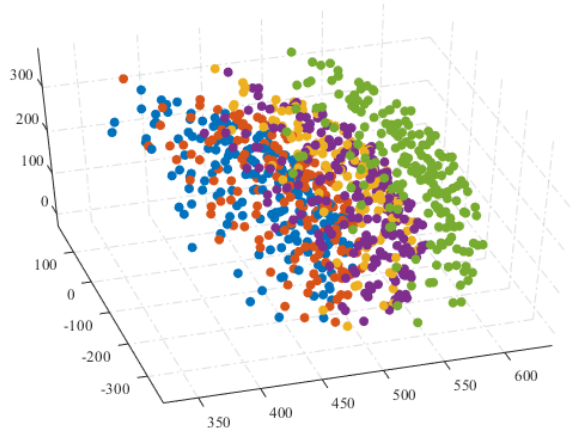

Fig. 5. Schematic diagram of Training Set

C. Control Experiment

To verify the effectiveness of the method, five controlled trials were conducted in this study. The conditions of each group are as follows. Group1 uses the deflection error model alone to compensate. Group 2 has a small training set and is compensated by neural networks alone. Group 3 has a large training set and is compensated by neural networks alone. Group 4 uses an improved kinematic solver with a deflection factor and is compensated by a neural network with a small training set. Group 5 uses an improved kinematic solver with a deflection factor and is compensated by a neural network with a large training set.

For the large deflection manipulator, the maximum error is from the Z direction. Table. I shows the average absolute value errors in the Z direction, which illustrates the effectiveness of the method. The average of variances from all directions is also shown in the third column. The compensation result is shown intuitively in Fig. 6.

TABLE I. RESULTS

Compensation Method	Absolute value of mean(mm)	Variance
Original error	17.7	223.94
Deflection only	15.39	215.97
SSA-BP only with 900 training set	5.32	52.83
SSA-BP only with 300 training set	12.66	214.37
Deflection +SSA-BP with 900 training set	5.79	57.15
Deflection +SSA-BP with 300 training set	9.98	180.81

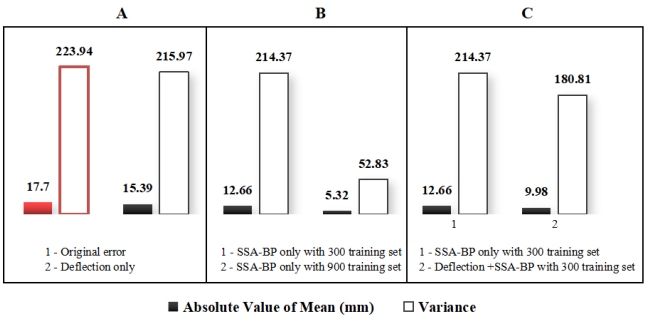

Fig. 6. Result Comparison

The accuracy of compensation is mainly determined by the accuracy of error estimation. According to comparison

Authorized licensed use limited to: Zhejiang University. Downloaded on April 27,2022 at 09:15:53 UTC from IEEE Xplore. Restrictions apply.

group A in Fig. 6, the control group which only uses the improved forward and inverse kinematics solver can compensate for the errors to a certain extent, which verifies the validity of the deflection modeling.

According to comparison group B in Fig. 6, when the training set is large, a better error fitting effect can be obtained, but the data collection time is more than 4 hours. However, when the size of the training set is 300, the fitting accuracy of the pure neural network decreases. The effectiveness of the error compensation by the neural network is verified.

This experiment especially focuses on the small training set. According to comparison group C in Fig. 6, when the training set is small, the result of using the improved solver which considers deflection is better than that of using the kinetic solver without optimization and the mean error is less than 10mm. The effectiveness of combining error model and neural network compensation in the case of difficult data collection is verified.

IV. Conclusion

In this paper, a universal compensation method for a large deflection manipulator is proposed. The innovation of this method lies in the combination of flexible error physical model and neural network compensation, and the long arm manipulator consistent with the rock drilling machine is designed for researchers to conduct research.

The result is better than compensation of independent flexible physical error modeling and independent neural network compensation, which makes up for the deficiency that physical error model is difficult to accurately model some error sources, and also solves the problem that neural network is not accurate enough in the case of fewer training samples. The combination of the traditional error model and the neural network can achieve the effect that the network does not need to be retrained under relatively loose conditions so that the adaptability to different working conditions is stronger.

The limitation of the study mainly lies in the difference between the simplified manipulator for the experiment and the real machine. Besides the data used for neural network training are insufficient and the number of control experiments is inadequate. In the future, the study will further improve the flexible error model, considering more error resources other than merely the deflection of the connecting rod. And the experiments will be conducted on real rock chisel machines to collect enough data in real engineering scenes and verify the compensation effect to apply the compensation method in the paper to automatic control of rock chisel.

Acknowledgment

National Natural Science Foundation of China (61836015) is acknowledged.

References

[1] Stieber M E, Mckay M, and Vukovich G, “Vision-based sensing and control for space robotics applications,” IEEE Transactions on Instrumentation & Measurement, vol.48, no.4, pp.807-812, 2002

[2] Peter J S, Sarjoun S and Chris U. Skyworker, “Assembly, Inspection, and Maintenance of Large Scale Orbital Facilities,” in The IEEE Conference on Robotics and Automation. Seoul, Korea, 2001, pp. 4180-4185.

[3] Guo Y, He Q H, and Zhu J X, “Computerized rock drill robot in tunneling,” Modern Tunnelling Technology, 2002

[4] Newman W S, Birkhimer C E, Horning R Jet al., “Calibration of a Motoman P8 robot based on laser tracking,” in SanFrancisco:IEEE International Conference on Robotics & Automation. IEEE, 2000, pp. 3597-3602

[5] Richter L, “Robust Real-Time Robot/Camera Calibration,” Robotized Transcranial Magnetic Stimulation, pp.63-84, 2013

[6] Khalil, Wisama , and Sébastien Besnard, “Geometric Calibration of Robots with Flexible Joints and Links,” Journal of Intelligent & Robotic Systems, vol.34, no.4, pp.357-379, 2002

[7] Huang Kaiqi, Wei Wenbin, Chen Ronghua, et al., “CEOPSO algorithm for positioning error compensation control of rock drilling robotic drilling arm,” Mechanical Science and Technology for Aerospace Engineering, vol. 37, no.7, pp.1005-1012, 2018

[8] Wang H S, Zhan D Y, and Huang P L, “Inverse kinematics of a heavy duty manipulator with 6-DOF based on dual quaternion,” Journal of Central South University, vol.022, no.007, pp.2568-2577, 2015

[9] Xia Y M, Ma Z S, and Zhang Y Z, “Bolting Jumbo Boom Positioning Based on Compliance Error Detection,” Journal of South China University of Technology, vol. 48, no. 3, pp.83-90, 2020

[10] Benallegue M, Lamiraux F, “Estimation and stabilization of humanoid flexibility deformation using only inertial measurement units and contact information,” International Journal of Humanoid Robotics, vol.12, no.3, 2015

[11] Tan Y S, Zhan D H, Zhang P H, “Analysis and Compensation of End Position Error of Rigid FlexibleCoupling Serial Manipulator,” Transactions of the Chinese Society for Agricultural Machinery, vol.52, no. 2, pp. 11.

[12] Wang Q, Bao W L, “Research on error compensation of drilling arm of rock-drilling robot based on GA-BP algorithm”. Mining & Processing Equipment, vol. 563, no.11, pp.6-10, 2020

[13] Hayati S A, “Robot arm geometric link parameter estimation” in IEEE Conference on Decision & Control. IEEE, 1983.

[14] Wang Lei, “Research on Kinematic Parameter Calibration and Precision Compensation Technology of Flexible Manipulator”. Beijing University of Posts and Telecommunications, 2019

[15] J. Xue, B. Shen, “A novel swarm intelligence optimization approach: sparrow search algorithm,” Systems Science & Control Engineering An Open Access Journal, vol. 8, no. 1, pp.22-34, 2020

[16] Wang X, Liu J, Hou T, “The SSA-BP-based potential threat prediction for aerialtarget considering commander emotion,” Defence Technology, vol. 3, 2021.

Authorized licensed use limited to: Zhejiang University. Downloaded on April 27,2022 at 09:15:53 UTC from IEEE Xplore. Restrictions apply.